Published in final edited form as:
Chemistry. 2014 November 3; 20(45): 14629–14632. doi:10.1002/chem.201405063.

Long-Lived Spin States for Low-Field Hyperpolarized Gas MRI

Dr. Kirill V. Kovtunov[a], **Dr. Milton L. Truong**[b], **Danila A. Barskiy**[a], **Prof. Igor V. Koptyug**[a], **Dr. Aaron M. Coffey**[b], **Prof. Kevin W. Waddell**[b], and **Prof. Eduard Y. Chekmenev**[b]

Eduard Y. Chekmenev: eduard.chekmenev@vanderbilt.edu

[a]Laboratory of Magnetic Resonance Microimaging, International Tomography Center, SB RAS, 3A Institutskaya St., Novosibirsk 630090 (Russia) and Novosibirsk State University, 2 Pirogova St., Novosibirsk 630090 (Russia)

[b]Institute of Imaging Science, Department of Radiology, Department of Biomedical Engineering, Department of Physics and Astronomy and Department of Biochemistry, Vanderbilt University, 1161 21st Ave South AA-1107, Nashville, TN, 37232-2310 (USA)

Abstract

Parahydrogen induced polarization was employed to prepare a relatively long-lived correlated nuclear spin state between methylene and methyl protons in propane gas. Conventionally, such states are converted into a strong NMR signal enhancement by transferring the reaction product to a high magnetic field in an adiabatic longitudinal transport after dissociation engenders net alignment (ALTADENA) experiment. However, the relaxation time T_1 of ~0.6 s of the resulting hyperpolarized propane is too short for potential biomedical applications. The presented alternative approach employs low-field MRI to preserve the initial correlated state with a much longer decay time T_{LLSS}=(4.7 ± 0.5) s. While the direct detection at low-magnetic fields (e.g. 0.0475 T) is challenging, we demonstrate here that spin-lock induced crossing (SLIC) at this low magnetic field transforms the long-lived correlated state into an observable nuclear magnetization suitable for MRI with sub-millimeter and sub-second spatial and temporal resolution, respectively. Propane is a non-toxic gas, and therefore, these results potentially enable low-cost high-resolution high-speed MRI of gases for functional imaging of lungs and other applications.

Keywords

gases; hyperpolarization; long-lived spin states; NMR imaging; propane

Hyperpolarization can increase the sensitivity of nuclear magnetic resonance by 4–6 orders of magnitude.[1] This increase in sensitivity enables the detection of dilute exogenous contrast media at low concentrations in vivo. The delivery of hyperpolarized (HP) contrast media by inhalation for functional and molecular imaging is particularly attractive, because of its convenience and relative non-invasiveness. To date, ^{3}He, ^{129}Xe, ^{131}Xe, and ^{83}Kr[2] were successfully hyperpolarized by the spin exchange optical pumping (SEOP) method,[3]

Correspondence to: Eduard Y. Chekmenev, eduard.chekmenev@vanderbilt.edu.

Supporting information for this article is available on the WWW under http://dx.doi.org/10.1002/chem.201405063.

and ^{3}He and ^{129}Xe[4] were successfully implemented in clinical trials. HP ^{3}He provides the highest sensitivity among noble gases because of its favorable nuclear spin properties, for example, gyromagnetic ratio γ_{3HE} which is only a factor of 1.32 smaller than that of a proton. However, due to the limited availability of ^{3}He, very high cost of ^{3}He, and its mandatory allocations for US Homeland security, it is unlikely to see a widespread biomedical use. The next most promising noble gas is ^{129}Xe, which can be hyperpolarized to the order unity on a clinical scale,[5] has a relatively high γ_{129XE} ~0.28×γ_{H}, and a relatively long in vivo gas-phase life time of hyperpolarization; that is, ^{129}Xe T_1 ~20 s.[4] Despite being very promising for imaging modalities capable of measuring lung function,[4] probing brain function,[6] and addressing events on the molecular and cellular level,[7] HP ^{129}Xe technology has several major obstacles for widespread clinical translation: i) its natural abundance is only ~26% and isotopic enrichment is frequently needed to maximize the payload of this contrast agent, ii) advanced high-cost SEOP hyperpolarization equipment (a hyperpolarizer) is required to produce relatively small quantities (~1–20 Lh^{-1}) of HP agents, iii) a customized MRI scanner with multinuclear capability and appropriate radio-frequency (rf) coils is required for ^{129}Xe imaging.[4] The last factor in particular has limited the distribution of this technology to only a few premier sites in the world.

A potential alternative to obviate the shortcomings of HP ^{129}Xe (and other noble gases) technology is the use of proton-based hyperpolarized contrast agents, which can be universally imaged by using conventional MRI scanners. While direct hyperpolarization of gaseous contrast agents is indeed feasible and has been demonstrated, very short relaxation times, T_1, of <1 s[8] cause the produced HP state of the gas to depolarize significantly faster compared to its handling and inhalation time, which requires at least several seconds. Figure 1 demonstrates preparation of HP propane using spin order of parahydrogen and adiabatic longitudinal transport after dissociation engenders net alignment (ALTADENA)[9] hyperpolarization technique, which results in two hyperpolarized (methylene and methyl) protons per each propane molecule. In this procedure, the singlet state of parahydrogen is first transferred by the chemical reaction to the product molecule at a very low (e.g. Earth's) magnetic field. The resulting state is then dissociated by adiabatic transfer of the product to a high magnetic field, which enables the detection of significantly enhanced absorptive (Ha, Figure 1B) and emissive (Hb, Figure 1B) NMR signals, because the difference in chemical shifts of two nascent protons at the detection field is significantly greater than their spin–spin coupling, that is, $\delta_{Ha}-\delta_{Hb} \gg J_{Ha-Hb}$.[9, 10] Despite efficient T_1 relaxation ($T_1(CH_2)$=(532 ± 6) ms and $T_1(CH_3)$=(616 ± 16) ms at 9.4 T), this ~1% HP contrast agent can be imaged under conditions of continuous flow,[11] with the depolarized gas being quickly replaced by the freshly produced agent. Figure 1D demonstrates an example of a true 3D MRI with very high spatial (0.5×0.5×0.5 mm^3 voxel size) and temporal (21.4 s scan duration) resolution with sensitivity approaching that of water, Figure 1 E.

A potential solution to extend the lifetime of HP propane is to populate its long-lived spin states (LLSS) using parahydrogen-induced polarization (PHIP), which can significantly increase relaxation times (as much as orders of magnitude).[12] Long-lived spin states of propane are created by the use of the low magnetic field of 0.0475 T, which is ~100 times lower than the 4.7 T field used to acquire the hyperpolarized propane image shown in Figure

1D, and ~30 times lower than the field of a 1.5 T clinical MRI scanner. The experimental setup shown in Figure 1C was used in the stopped-flow regime for low-field NMR studies, where the HP propane gas was stopped inside an ~2 mL cavity placed in a 0.0475 T MRI scanner. The direct detection of the resulting NMR spectrum, Figure 2D, gives the signal with an antiphase pattern. However, this signal is approximately 2–3 orders of magnitude lower than the expected value based on $\%P_H$ ~1% measured at 4.7 T.[13] At the same time, the spin states responsible for this signal are significantly longer lived with T_{LLSS}=(4.7 ± 0.5) s. These observations show that under the low field conditions ($\delta_{Ha}-\delta_{Hb} \ll J_{Ha-Hb}$) the initial singlet spin state of parahydrogen populates long-lived spin states of propane while creating only a small directly observable magnetization. Thus, the direct detection in such experiments is clearly disadvantageous because it gives low SNR in the acquired spectra and images. At the same time, the increase in the lifetime of hyperpolarization T_{LLSS} ~4.7 s is clearly attractive, because it is now sufficient for gas delivery and inhalation.[2] For example, this value of T_{LLSS} is substantially larger than the T_1 of HP ^{83}Kr in vivo of <2 s,[14] which has already been pursued as a potential in vivo contrast agent[2].

A detailed analysis of the spectrum of Figure 2D shows that the outer antiphase peaks are in fact the ^{13}C satellites arising due to the one-bond J_{H-13C} couplings in those propane molecules that contain ^{13}C nuclei (see Supporting Information for details). As the natural abundance of the ^{13}C isotope is only 1.1 %, it can be concluded that the signal enhancement for the ^{13}C satellites is in fact much larger than for propane molecules containing no ^{13}C nuclei.[15] Therefore, isotopic enrichment with ^{13}C could potentially lead to much larger signal enhancements in such experiments. Clearly, this approach would be too expensive for high-throughput MRI, and in addition would provide little control for manipulating the hyperpolarization in an NMR experiment. Nevertheless, observation of the strongly enhanced ^{13}C satellites in this spectrum shows that much larger signal enhancements should be possible to achieve in such experiments.

A number of rf pulse-sequences were recently developed for transforming the NMR hyperpolarization stored in the long-lived (singlet) (LLS) spin states into observable nuclear magnetization.[16] Here, spin-lock induced crossing (SLIC) based rf pulse sequence developed by Rosen and co-workers[16c] was employed to convert the LLSS prepared in the Earth's magnetic field into the significantly enhanced observable magnetization at 47.5 mT (Figure 3). As a result, a significantly greater (~2 orders of magnitude) NMR signal was detected in Figure 3C compared to that in Figure 2D. The enhancement of nuclear spin polarization ε was ~5100 corresponding to an absolute nuclear spin polarization $\%P_H$ ~0.08% per each nascent proton. A spectrum of thermally polarized water with ~10^3 greater molar quantity (Figure 3D) was used for signal referencing purposes, because recording of propane thermal NMR spectrum would be impractical due to very low thermal signal. The estimated $\%P_H$ is notably reduced compared to $\%P_H$ ~1% observed in high-field studies (Figure 1B). The decrease in apparent nuclear spin polarization is in part due to the relaxation during the ~2 s-long B_1 spin-lock. Furthermore, the SLIC procedure was not fully optimized and was performed under conditions of very low rf power decoupling, which is challenging, because of non-linearity and the high noise figure of high-power rf amplifiers in the μW regime, which can be potentially mitigated in the future by using more advanced

SLIC sequences with adiabatic rf pulses.[17] While the relaxation losses are difficult to avoid, the choice of power-optimized rf hardware and further rf pulse sequence optimization can potentially minimize hyperpolarization losses.

The proof-of-principle sub-second MRI with HP propane produced using this approach is shown in Figure 3 E and a corresponding image of thermally polarized water is presented in Figure 3 F. These images were acquired at 0.0475 T using MRI rf coil[18] with ~40% sensitivity of 4.7 T MRI coils such as that used for MRI presented in Figure 1D. In principle, the sensitivity of low-field MRI can surpass high-field MRI sensitivity for detection of hyperpolarized contrast agents including HP propane studied here[18].

The quality (speed, SNR and spatial resolution) of GRE images presented in Figure 1D and 3E should not be compared directly, because the image presented in Figure 1D is enhanced by i) rf excitation pulses with a greater flip angle, ii) 192 times more encoding steps, iii) a more sensitive rf coil, and iv) flowing propane gas that constantly replenishes hyperpolarization during imaging. Nevertheless, the image with a 0.88×0.88 mm^2 in-plane spatial resolution was demonstrated in ~0.7 s total acquisition time (Figure 3 E), which was largely limited by electronics response time of the receiver. 3D MRI of HP propane on a time scale of seconds is feasible using 3.48 ms repetition time (Figure 1D) and compressed sensing image encoding, which has been already shown to accelerate HP MRI by 3–4 fold and can potentially achieve more than an order of magnitude increase in temporal resolution.[19] Furthermore, ultra-fast (<5 s) 3D MRI of patient lungs on a single breath-hold with HP ^{129}Xe has been demonstrated with <25% hyperpolarized ^{129}Xe without compressed sensing.[5] HP propane and potentially other gaseous HP ^{1}H contrast agents offer multiple significant advantages over HP noble gases and other HP heteronuclear contrast agents[20] even under conditions of nominally lower hyperpolarization levels. First, each HP propane molecule carries a double payload of hyperpolarization compared to monoatomic HP ^{129}Xe, ^{3}He, ^{83} Kr and other gases. Second, protons have the highest nuclear gyromagnetic ratio γ_H. For example, γ_H is 3.6 times greater than γ_{129XE}. Third, proton spins have nearly 100% natural abundance, while ^{129}Xe natural abundance is 26%, and is much lower for ^{3}He and ^{83}Kr. These compounding factors make ^{129}Xe detection more than 27 times less sensitive than ^{1}H detection. There are other practical challenges of low-γ nuclei detection: i) the requirement of specialized and costly hardware, which is not universally available, and ii) significantly higher gradient power (proportional to the square of the ratio of gyromagnetic ratios of proton and low-γ nucleus) requirements[20] and iii) contrast agent cost. The above advantages make this low-cost HP propane a very promising contrast agent for potential biomedical and other uses. Propane is a non-toxic asphyxiating gas (i.e. it is relatively inert when administered in vivo; moreover, it has no observed developmental or systemic effects even under high (10000 ppm) concentration as studied in a recent randomized 90 day inhalation toxicity study[21]), and has a widespread use in cosmetics, foods (as a propellant), and other uses.[22] Moreover, PHIP is a relatively simple and not instrumentation-demanding method requiring only parahydrogen, propene and a special solid-phase recyclable heterogeneous catalyst. Notably, a heterogeneous solid-state catalyst was used to prepare pure HP propane gas, which can be used without additional purification steps, although implementation of in-line filters to capture any residual catalyst nanoparticles may be warranted in the design of future propane hyperpolarization equipment

similarly to SEOP ^{129}Xe hyperpolarizers.[5, 23] Delivery and inhalation of HP propane would require several seconds rendering the prospective biomedical use potentially feasible due to sufficiently long relaxation time T_{LLSS}, although future in vivo demonstration studies would be required to prove in vivo feasibility. Moreover, prospective in vivo studies would likely require a dedicated robust hyperpolarizer similar to hyperpolarizers[1, 4, 5] needed for pre-clinical and clinical translation of DNP and SEOP hyperpolarized contrast agents. The transformation of the LLSS of propane into the observable signal was achieved with just 36 μW of rf power in a 38 mm ID rf coil (corresponding to B_1 nutation frequency of (10 ± 5) Hz); scaling to a human subject size will likely require less than a Watt of rf power with negligible specific absorption rate (SAR) at low resonance frequencies,[24] making it a very safe procedure.

The catalyst allowed an efficient addition of parahydrogen gas to propene (Figure 1A), although the molecular addition pathway likely represents only a small fraction (a few percent) of overall hydrogenation yield. Improving the yield of heterogeneous hydrogenation and especially of the pairwise addition pathway, handling of HP propane, and MR preparation and imaging sequences can potentially further improve the detection MRI sensitivity of HP propane by 1–3 orders of magnitude to a level enabling sensitive high-resolution MRI of lungs and other applications with sub-second temporal resolution.

Experimental Section

Experimental Details are provided in the Supporting Information.

Supplementary Material

Refer to Web version on PubMed Central for supplementary material.

Acknowledgments

This work was supported by the RAS (5.1.1), RFBR (14-03-00374-a, 14–03–31239-mol-a, 12–03–00403-a), SB RAS (57, 60, 61, 122), the Ministry of Education and Science of the Russian Federation, and the grants MK-4391.2013.3, NIH ICMIC 5P50 CA128323–03, NIGMS 1R21 GM107947–01, 5R00 CA134749–03, 3R00A134749–02S1, US DoD CDMRP W81XWH-12-1-265 0159/BC112431.

References

1. Ardenkjaer-Larsen JH, Fridlund B, Gram A, Hansson G, Hansson L, Lerche MH, Servin R, Thaning M, Golman K. Proc Natl Acad Sci USA. 2003; 100:10158–10163. [PubMed: 12930897]
2. Lilburn D, Pavlovskaya GE, Meersmann T. J Magn Reson. 2013; 229:173–186. [PubMed: 23290627]
3. Walker TG, Happer W. Rev Mod Phys. 1997; 69:629–642.
4. Mugler JP, Altes TA. J Magn Reson Imaging. 2013; 37:313–331. [PubMed: 23355432]
5. Nikolaou P, Coffey AM, Walkup LL, Gust BM, Whiting N, Newton H, Barcus S, Muradyan I, Dabaghyan M, Moroz GD, Rosen M, Patz S, Barlow MJ, Chekmenev EY, Goodson BM. Proc Natl Acad Sci USA. 2013; 110:14150–14155. [PubMed: 23946420]
6. Goodson BM. J Magn Reson. 2002; 155:157–216. [PubMed: 12036331]
7. Schroder L, Lowery TJ, Hilty C, Wemmer DE, Pines A. Science. 2006; 314:446–449. [PubMed: 17053143]

8. Kovtunov KV, Zhivonitko VV, Skovpin IV, Barskiy DA, Koptyug IV. Top Curr Chem. 2012; 338:123–180. [PubMed: 23097028]
9. Pravica MG, Weitekamp DP. Chem Phys Lett. 1988; 145:255–258.
10. We note that, strictly speaking, this qualitative model is correct only for a 2-spin system. For an 8-spin system of propane the situation is significantly more complicated, but it still reflects qualitatively the essence of the underlying physics.
11. Bouchard LS, Burt SR, Anwar MS, Kovtunov KV, Koptyug IV, Pines A. Science. 2008; 319:442–445. [PubMed: 18218891]
12. Carravetta M, Levitt MH. J Am Chem Soc. 2004; 126:6228–6229. [PubMed: 15149209]
13. Kovtunov KV, Barskiy DA, Coffey AM, Truong ML, Salnikov OG, Khudorozhkov AK, Inozemceva EA, Prosvirin IP, Bukhtiyarov VI, Waddell KW, Chekmenev EY, Koptyug IV. Chem Eur J. 2014; 20:11636–11639. [PubMed: 24961814]
14. Six JS, Hughes-Riley T, Lilburn DML, Dorkes AC, Stupic KF, Shaw DE, Morris PG, Hall IP, Pavlovskaya GE, Meersmann T. Magn Reson Imaging. 2014; 32:48–53. [PubMed: 24144493]
15. Colell J, Turschmann P, Gloggler S, Schleker P, Theis T, Ledbetter M, Budker D, Pines A, Blumich B, Appelt S. Phys Rev Lett. 2013; 110:5.
16. a) Pileio G, Carravetta M, Hughes E, Levitt MH. J Am Chem Soc. 2008; 130:12582–12583. [PubMed: 18729363] b) Warren WS, Jenista E, Branca RT, Chen X. Science. 2009; 323:1711–1714. [PubMed: 19325112] c) DeVience SJ, Walsworth RL, Rosen MS. Phys Rev Lett. 2013; 111:5.
17. Theis T, Feng Y, Wu T, Warren WS. J Chem Phys. 2014; 140:7.
18. Coffey AM, Truong ML, Chekmenev EY. J Magn Reson. 2013; 237:169–174. [PubMed: 24239701]
19. a) Larson PEZ, Hu S, Lustig M, Kerr AB, Nelson SJ, Kurhanewicz J, Pauly JM, Vigneron DB. Magn Reson Med. 2011; 65:610–619. [PubMed: 20939089] b) Sarracanie M, Armstrong BD, Stockmann J, Rosen MS. Magn Reson Med. 2014; 71:735–745.
20. Kurhanewicz J, Vigneron DB, Brindle K, Chekmenev EY, Comment A, Cunningham CH, DeBerardinis RJ, Green GG, Leach MO, Rajan SS, Rizi RR, Ross BD, Warren WS, Malloy CR. Neoplasia. 2011; 13:81–97. [PubMed: 21403835]
21. McKee RH, Herron D, Saperstein M, Podhasky P, Hoffman GM, Roberts L. Int J Toxicol. 2014; 33:28S–51S. [PubMed: 24179026]
22. Hijazi R, Taylor D, Richardson J. Br Med J. 2009; 338:5.
23. Nikolaou P, Coffey AM, Walkup LL, Gust B, LaPierre C, Koehnemann E, Barlow MJ, Rosen MS, Goodson BM, Chekmenev EY. J Am Chem Soc. 2014; 136:1636–1642. [PubMed: 24400919]
24. Hayden ME, Bidinosti CP, Chapple EM. Concept Magnetic Res A. 2012; 40:281–294.

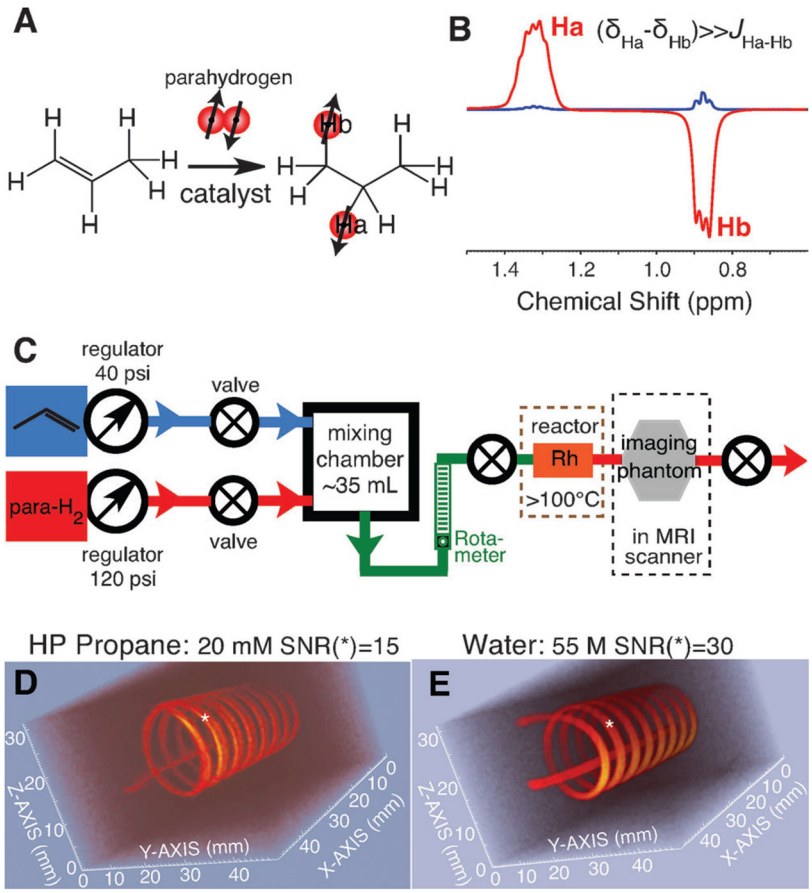

Figure 1.

NMR spectroscopy and MRI of ALTADENA HP propane under continuous flow conditions. A) Reaction scheme of molecular addition of parahydrogen to propene resulting in HP propane, B) high-resolution ALTADENA NMR spectroscopy of continuously flowing HP propane gas at 9.4 T, C) schematics of ALTADENA experimental setup for HP propane detection at 4.7 T MRI and 9.4 T NMR, D) 3D gradient echo (GRE) imaging of continuously flowing HP propane at 4.7 T, E) corresponding image of still water. Both images were acquired with 0.5×0.5×0.5 mm^3 spatial voxel size resolution in 21.4 s.

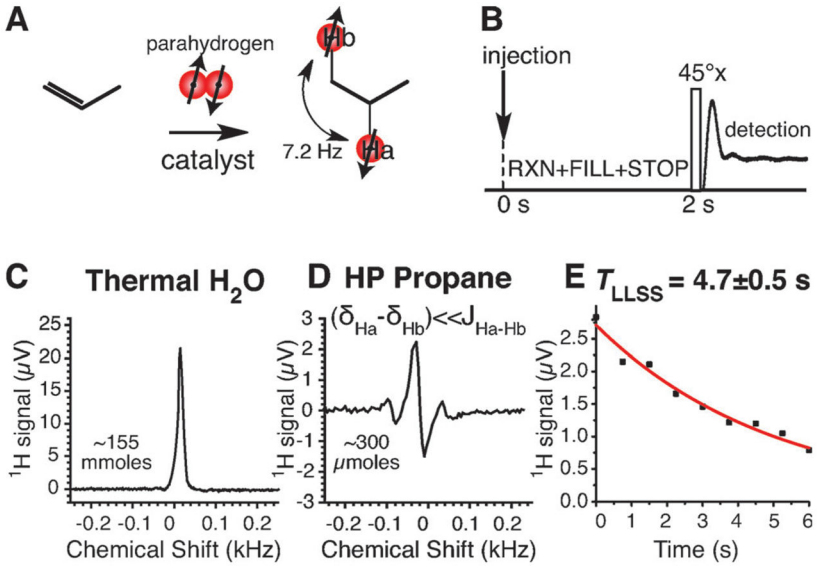

Figure 2.

Low-field single-scan NMR spectroscopy at 0.0475 T; A) the diagram of molecular addition of parahydrogen gas to propene resulting in HP propane, B) the sequence of events, C) single-scan reference spectrum of 2.8 mL water acquired with a 45° excitation rf pulse, D) single-scan reference spectrum of HP propane (prepared in the Earth's magnetic field and then transferred to 47.5 mT) obtained using the protocol depicted in (B) and the same acquisition parameters as in (C), E) The LLSS relaxation decay T_{LLSS} of HP propane correlated spin state monitored by 7° excitation rf pulse every 0.75 s.

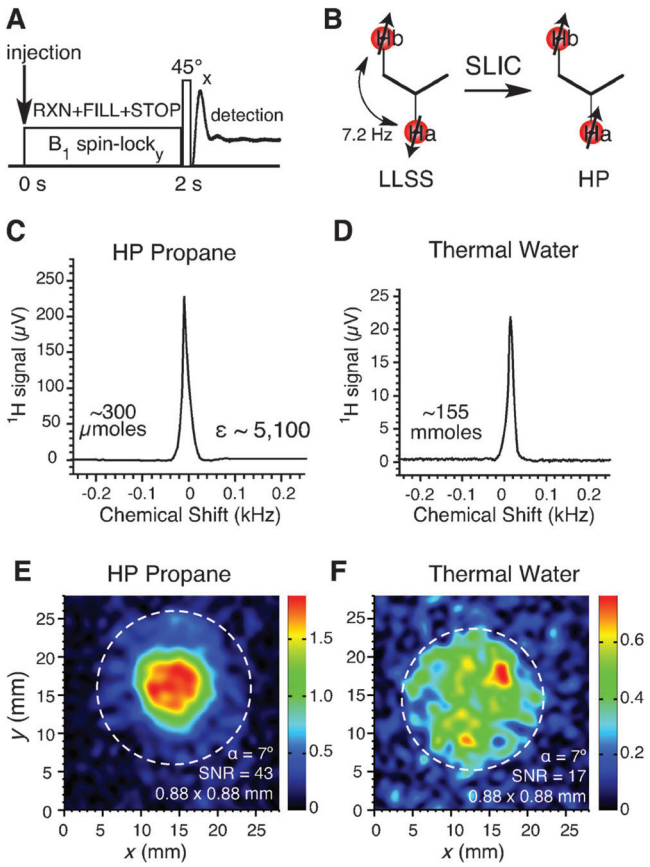

Figure 3.

NMR studies of HP propane irradiated with continuous wave (CW) decoupling at 2.0 MHz (B_0=0.0475 T) using SLIC.[16c] A) Sequence of events including SLIC block of B_1 spin-lock; B) schematics of propane correlated state conversion to the observable hyperpolarization via SLIC pulse-sequence block, C) ^{1}H spectrum detected using the sequence described above, D) Corresponding NMR signal reference spectrum of thermally polarized water; E) 2D gradient echo (GRE) imaging of HP propane (without slice selection) using the following imaging parameters: TE/TR=7.0/20 ms, acquisition time=6.4 ms, spectral width (SW)=5.0 kHz, rf excitation pulse (α)=7° (6.0 μs), field of view (FOV)=28×28 mm^2 using 32×32 imaging matrix with 2 dummy scans with total imaging time of ~0.7 s. An estimated %P_H was ~0.04% at the beginning of imaging sequence. The disc (dashed circle) highlights the wider (but thinner) section of the 2 mL phantom. Note more intense central region of the image due to greater reservoir thickness. F) A corresponding image of thermally polarized water. Dashed circle identifies the 1.75 cm-diameter of 2.8 mL sphere of water. No compressed sensing was used, and signal-to-noise ratio (SNR) of the maximum voxel SNR was 43 in (E) and 17 in (F) respectively. Both images were extrapolated to 1024×1024 pixels to enhance visual representation.